Cosmological constraints on ghost dark energy in the Brans–Dicke theory by using MCMC approach

Hamzeh Alavirad [a], Ahmad Sheykhi [b,c,*]

[a] *Institute for Theoretical Physics, Karlsruhe Institute of Technology (KIT), 76128 Karlsruhe, Germany*
[b] *Physics Department and Biruni Observatory, College of Sciences, Shiraz University, Shiraz 71454, Iran*
[c] *Research Institute for Astronomy and Astrophysics of Maragha (RIAAM), P.O. Box 55134-441, Maragha, Iran*

A B S T R A C T

By using a Markov Chain Monte Carlo simulation, we investigate cosmological constraints on the ghost dark energy (GDE) model in the framework of the Brans–Dicke (BD) theory. A combination of the latest observational data of the cosmic microwave background radiation data from seven-year WMAP, the baryon acoustic oscillation data form the SDSS, the supernovae type Ia data from the Union2 and the X-ray gas mass fraction data from the Chandra X-ray observations of the largest relaxed galaxy clusters are used to perform constraints on GDE in the BD cosmology. In this paper, we consider both flat and non-flat universes together with interaction between dark matter and dark energy. The main cosmological parameters are obtained as: $\Omega_b h^2 = 0.0223^{+0.0016}_{-0.0013}$, $\Omega_c h^2 = 0.1149^{+0.0088}_{-0.0104}$ and $\Omega_k = 0.0005^{+0.0025}_{-0.0073}$. In addition, the Brans–Dicke parameter ω is estimated as $1/\omega \simeq 0.002$.

1. Introduction

Accelerating expansion of the Universe [1,2] can be explained either by a missing energy component usually called "dark energy" (DE) with an exotic equation of state, or by modifying the underlying theory of gravity on large scales. The famous examples of the former approach include scalar field models of DE such as quintessence [3,4], K-essence [5,6], tachyon [7,8], phantom [9–11], ghost condensate [12,13], quintom [14–16], holographic DE [17], agegraphic DE [18,19] and so forth. For a comprehensive review on DE models, see [20,21]. The latter approach for explanation of the acceleration expansion is based on the modification of the underlying theory of gravity on large scales such as $f(R)$ gravity [22] and braneworld scenarios [23–26].

Among various models of DE, the so called ghost dark energy (GDE) has attracted a lot of interest in recent years. The origin of DE in this model comes from Veneziano ghosts in QCD theory [27–30]. Indeed, the contribution of the ghosts field to the vacuum energy in curved space or time-dependent background can be regarded as a possible candidate for DE [31,32]. The magnitude of this vacuum energy is of order $\Lambda_{QCD}^3 H$, where H is the Hubble pa-

rameter and Λ_{QCD} is the QCD mass scale. With $\Lambda_{QCD} \sim 100$ MeV and $H \sim 10^{-33}$ eV, $\Lambda_{QCD}^3 H$ gives the right order of magnitude $\sim (3 \times 10^{-3}$ eV$)^4$ for the observed dark energy density [31]. The advantages of GDE model compared to other DE models is that it is totally embedded in standard model and general relativity, therefore one needs not to introduce any new parameter, new degree of freedom or to modify gravity. The dynamical behavior of GDE model in flat universe have been studied [33]. The study was also generalized to the universe with spacial curvature [34]. The instability of the GDE model against perturbations was studied in [35]. In [36,37] the correspondence between GDE and scalar field models of DE was established. In the presence of bulk viscosity and varying gravitational constant, the GDE model was investigated in [38]. Other features of the GDE model have been investigated in Refs. [39–43]. The cosmological constraints on this model have been considered by some authors [33,43,44].

Recently, scalar tensor theories have been reconsidered extensively. One important example of the scalar tensor theories is the BD theory of gravity which was introduced by Brans and Dicke in 1961 to incorporate Mach's principle in Einstein's theory of gravity [45]. This theory also passes the observational tests in the solar system domain [46]. In addition, BD theory can be tested by the cosmological observations such as the cosmic microwave background (CMB) and large scale structure (LSS) [47–51]. Since the GDE model has a dynamic behavior, it is more reasonable to consider this model in a dynamical framework such as BD theory.

It was shown that some features of GDE in BD cosmology differ from Einstein's gravity [52]. For example, while the original DE is instable in all range of the parameter spaces in standard cosmology [35], it leads to a stable phase in BD theory [53]. In the framework of BD cosmology, the ghost model of DE has been studied [52]. It is also of great interest to see whether the GDE model in the framework of the BD theory is compatible with observational data or not.

In this paper, cosmological constraints on GDE in the BD theory (GDEBD) [52] theory is performed by using the Marko Chain Monte Carlo (MCMC) simulation. The used observational datasets are as follows: cosmic microwave background radiation (CMB) from WMAP7 [54], 557 Union2 dataset of type Ia supernova [55], baryon acoustic oscillation (BAO) from SDSS DR7 [56], and the cluster X-ray gas mass fraction from the Chandra X-ray observations [57]. To put the constraints, the modified CosmoMC [58] code is used.

The organization of this paper is as follows. In Section 2, we review the formalism of the GDE in the framework of Brans–Dicke cosmology. In Section 3 the methods which are used in this paper to analyze the data are introduced. Section 4 contains the results of the MCMC simulation and we conclude our paper in Section 5.

2. Interacting ghost dark energy in the Brans–Dicke theory in a non-flat universe

Let us first review the formalism of the interacting GDE in the framework of BD theory in a non-flat universe [52]. The action of the BD theory in the canonical form may be written [59]

$$S = \int d^4x \sqrt{g} \left(-\frac{1}{8\omega}\phi^2 R + \frac{1}{2}g^{\mu\nu}\partial_\mu\phi\partial_\nu\phi + L_M \right), \tag{1}$$

where R is the Ricci scalar and ϕ is the BD scalar field. Varying the action with respect to the metric $g_{\mu\nu}$ and the BD scalar field ϕ, yields

$$\phi G_{\mu\nu} = -8\pi T^M_{\mu\nu} - \frac{\omega}{\phi}\left(\phi_{,\mu}\phi_{,\nu} - \frac{1}{2}g_{\mu\nu}\phi_{,\lambda}\phi^{,\lambda}\right)$$
$$\quad - \phi_{;\mu;\nu} + g_{\mu\nu}\Box\phi, \tag{2}$$

$$\Box\phi = \frac{8\pi}{2\omega+3}T^{M\lambda}_\lambda, \tag{3}$$

where $T^M_{\mu\nu}$ stands for the energy-momentum tensor of the matter fields. The line element of the Friedmann–Robertson–Walker (FRW) universe is

$$ds^2 = dt^2 - a^2(t)\left(\frac{dr^2}{1-kr^2} + r^2 d\Omega^2\right), \tag{4}$$

where $a(t)$ is the scale factor, and k is the curvature parameter with $k = -1, 0, 1$ corresponding to open, flat, and closed universes, respectively. Nowadays, there are some evidences in favor of closed universe with a small positive curvature ($\Omega_k \simeq 0.01$) [61]. Using metric (4), the field Eqs. (2) and (3) reduce to

$$\frac{3}{4\omega}\phi^2\left(H^2 + \frac{k}{a^2}\right) - \frac{1}{2}\dot{\phi}^2 + \frac{3}{2\omega}H\dot{\phi}\phi = \rho_m + \rho_D, \tag{5}$$

$$\frac{-1}{4\omega}\phi^2\left(2\frac{\ddot{a}}{a} + H^2 + \frac{k}{a^2}\right) - \frac{1}{\omega}H\dot{\phi}\phi - \frac{1}{2\omega}\ddot{\phi}\phi - \frac{1}{2}\left(1 + \frac{1}{\omega}\right)\dot{\phi}^2$$
$$\quad = p_D, \tag{6}$$

$$\ddot{\phi} + 3H\dot{\phi} - \frac{3}{2\omega}\left(\frac{\ddot{a}}{a} + H^2 + \frac{k}{a^2}\right)\phi = 0, \tag{7}$$

where $H = \dot{a}/a$ is the Hubble parameter, ρ_D and p_D are, respectively, the energy density and pressure of DE, and ρ_m is the pressureless matter density which contains both dark matter (DM) and baryonic matter (BM) densities i.e. $\rho_m = \rho_c + \rho_b$ where ρ_c and ρ_b are the energy densities of dark matter and baryonic matter respectively.

To be more general and because of some observational evidences [62,63], here we propose the case where there is an interaction between GDE and DM. In this case the semi-conservation equations read

$$\dot{\rho}_D + 3H\rho_D(1 + w_D) = -Q, \tag{8}$$

$$\dot{\rho}_c + 3H\rho_c = Q, \tag{9}$$

$$\dot{\rho}_b + 3H\rho_b = 0, \tag{10}$$

where Q represents the interaction term between dark matter and dark energy and here we assume that the baryonic matter is conserved separately. We assume $Q = 3\xi H(\rho_m + \rho_D)$ with ξ being a constant. Such a choice for interacting term implies the DE and DM component do not conserve separately while the total density is still conserved through

$$\dot{\rho} + 3H(\rho + P) = 0, \tag{11}$$

where $\rho = \rho_D + \rho_m$ and $P = P_D$.

The ghost energy density is proportional to the Hubble parameter [31]

$$\rho_D = \alpha H, \tag{12}$$

where $\alpha > 0$ is roughly of order Λ^3_{QCD} and Λ_{QCD} are QCD mass scale. Taking into account the fact that $\Lambda_{QCD} \sim 100$ MeV and $H \sim 10^{-33}$ eV for the present time, this gives the right order of magnitude $\rho_D \sim (3 \times 10^{-3} \text{ eV})^4$ for the ghost energy density [31].

Since the system of Eqs. (5)–(7) is not closed, we still have another degree of freedom in analyzing the set of equations. As usual we assume the BD scalar field ϕ has a power law relation versus the scale factor,

$$\phi = \phi_0 a(t)^\varepsilon. \tag{13}$$

An interesting case is when ε is small whereas ω is high so that the product $\varepsilon\omega$ results of order unity [64,65]. In Section 4 we will consider the $\omega\varepsilon = 1$ condition for constraining the model by observational data. This is interesting because local astronomical experiments set a very high lower bound on ω [66]; in particular, the Cassini experiment implies that $\omega > 10^4$ [46,48]. Now we take the time derivative of relation (13). We arrive at

$$\frac{\dot{\phi}}{\phi} = \varepsilon\frac{\dot{a}}{a} = \varepsilon H. \tag{14}$$

Combining Eqs. (13) and (14) with the first Friedmann equation (5), we get

$$H^2\left(1 - \frac{2\omega}{3}\varepsilon^2 + 2\varepsilon\right) + \frac{k}{a^2} = \frac{4\omega}{3\phi^2}(\rho_D + \rho_m). \tag{15}$$

As usual the fractional energy densities are defined as

$$\Omega_c = \frac{\rho_c}{\rho_{cr}} = \frac{4\omega\rho_c}{3\phi^2 H^2}, \tag{16}$$

$$\Omega_b = \frac{\rho_b}{\rho_{cr}} = \frac{4\omega\rho_b}{3\phi^2 H^2}, \tag{17}$$

$$\Omega_k = \frac{\rho_k}{\rho_{cr}} = \frac{k}{H^2 a^2}, \tag{18}$$

$$\Omega_D = \frac{\rho_D}{\rho_{cr}} = \frac{4\omega\rho_D}{3\phi^2 H^2}, \tag{19}$$

where

$$\rho_{\text{cr}} = \frac{3\phi^2 H^2}{4\omega}. \tag{20}$$

Using (12) we can rewrite Eq. (19) as

$$\Omega_{\text{D}} = \frac{4\omega\alpha}{3\phi^2 H}. \tag{21}$$

Based on these definitions, Eq. (15) can be rewritten as

$$\gamma = \Omega_{\text{D}} + \Omega_{\text{m}} - \Omega_k, \tag{22}$$

where $\Omega_{\text{m}} = \Omega_{\text{c}} + \Omega_{\text{b}}$ and we have defined

$$\gamma = 1 - \frac{2\omega}{3}\varepsilon^2 + 2\varepsilon. \tag{23}$$

Next we take the time derivative of (15), after using (22), we find

$$\frac{\dot{H}}{H^2} = \frac{\Omega_k}{\gamma} - \left(1 + \frac{\Omega_k}{\gamma}\right)\left[\varepsilon + \frac{3}{2} + \frac{3}{2}\frac{\Omega_{\text{D}} w_{\text{D}}}{\gamma + \Omega_k}\right]. \tag{24}$$

Combining the above equation with Eqs. (8) and (12), we obtain the EoS parameter as

$$w_{\text{D}} = -\frac{\gamma}{2\gamma - \Omega_{\text{D}}}\left(1 - \frac{\Omega_k}{3\gamma} - \frac{2\varepsilon}{3}\left(1 + \frac{\Omega_k}{\gamma}\right)\right.$$
$$\left. + \frac{2\xi}{\Omega_{\text{D}}}(\gamma + \Omega_k - \Omega_{\text{b}})\right). \tag{25}$$

The first and second derivatives of the distance can be combined to obtain the acceleration parameter q. It was shown that the zero redshift value of q_0, is independent of space curvature, and can be obtained from the first and second derivatives of the coordinate distance [67]. It was argued that q_0, which indicates whether the universe is accelerating at the current epoch, can be obtained directly from the supernova and radio galaxy data [67]. The acceleration parameter is given by

$$q = -1 - \frac{\dot{H}}{H^2}. \tag{26}$$

Using (24) the acceleration parameter (26) is obtained as

$$q = \left(1 + \frac{\Omega_k}{\gamma}\right)\left[\epsilon + \frac{1}{2}\right] + \frac{\Omega_{\text{D}}\epsilon}{2\gamma - \Omega_{\text{D}}}$$
$$- \frac{3\Omega_{\text{D}}}{2(2\gamma - \Omega_{\text{D}})}\left[1 - \frac{\Omega_k}{3\gamma} + \frac{2\xi}{\Omega_{\text{D}}}(\gamma + \Omega_k - \Omega_{\text{b}})\right]. \tag{27}$$

Finally, we obtain the equation of motions of GDE in BD theory. For this purpose, we first take the time derivative of relation (21). We find

$$\dot{\Omega}_{\text{D}} = \Omega_{\text{D}} H(1 + q - 2\varepsilon). \tag{28}$$

Substituting q from (27) into Eq. (28) and using relation $\Omega'_{\text{D}} = H\frac{d\Omega_{\text{D}}}{d\ln a}$, we get

$$\frac{d\Omega_{\text{D}}}{d\ln a} = \Omega_{\text{D}}\left[1 + \left(1 + \frac{\Omega_k}{\gamma}\right)\left[\epsilon + \frac{1}{2}\right] + \frac{\Omega_{\text{D}}\epsilon}{2\gamma - \Omega_{\text{D}}}\right.$$
$$\left. - \frac{3\Omega_{\text{D}}}{2(2\gamma - \Omega_{\text{D}})}\left[1 - \frac{\Omega_k}{3\gamma} + \frac{2\xi}{\Omega_{\text{D}}}(\gamma + \Omega_k - \Omega_{\text{b}})\right] - 2\varepsilon\right]. \tag{29}$$

In the remaining part of this paper we will constrain the GDEBD model by using the most recent observational date in the three different physical models: model I which is the GDEBD model in a flat universe ($\xi = 0$ and $\Omega_k = 0$), model II is the interacting GDEBD model in a flat universe ($\xi \neq 0$ and $\Omega_k = 0$) and finally model III is the interacting GDEBD model in a non-flat universe ($\xi \neq 0$ and $\Omega_k \neq 0$).

3. Data fitting method

In this section we discuss the data fitting method in the Markov Chain Monte Carlo (MCMC) simulation to estimate the parameters of the model in Section 2 using cosmological data.

To get the best fit values of the relevant parameters, the maximum likelihood method is used. The total likelihood function $\mathcal{L}_{\text{total}} = e^{-\chi^2_{\text{tot}}/2}$ is defined as the product of the separate likelihood functions of uncorrelated observational data with

$$\chi^2_{\text{tot}} = \chi^2_{\text{SNIa}} + \chi^2_{\text{CMB}} + \chi^2_{\text{BAO}} + \chi^2_{\text{gas}}, \tag{30}$$

where SNIa stands for type Ia supernovae, CMB for cosmic microwave background radiation, BAO for baryon acoustic oscillation and *gas* stands for X-ray gas mass fraction data. Best fit values of parameters are obtained by minimizing χ^2_{tot}. In this paper we use the cosmic microwave background radiation data from seven-year WMAP [54], type Ia supernovae data from 557 Union2 [55], baryon acoustic oscillation data from SDSS DR7 [56], and the cluster X-ray gas mass fraction data from the Chandra X-ray observations [57]. In the rest of this section we discuss each χ^2_i in detail.

To obtain χ^2_{CMB}, we use seven-year WMAP data [54] with the CMB data point (R, l_A, z_*). The shift parameter R, which parametrize the changes in the amplitude of the acoustic peaks is given by [68]

$$R = \sqrt{\frac{\Omega_{\text{m0}}}{c}} \int_0^{z_*} \frac{dz'}{E(z')}, \tag{31}$$

where z_* is the redshift of recombination (see (36)), c is the speed of light in vacuum, Ω_{m0} is the present value of the matter density parameter (a "0" subscript shows the present value of the related quantity), and $E(z) \equiv H(z)/H_0$. In addition, the acoustic scale l_A, which characterizes the changes of the peaks of CMB via the angular diameter distance out to recombination is defined as [68]

$$l_A = \frac{\pi r(z_*)}{r_s(z_*)}. \tag{32}$$

The comoving distance $r(z)$ is defined

$$r(z) = \frac{c}{H_0} \int_0^z \frac{dz'}{E(z')}, \tag{33}$$

and the comoving sound horizon distance at recombination $r_s(z_*)$ is given by

$$r_s(z_*) = \int_0^{a(z_*)} \frac{c_s(a)}{a^2 H(a)} da, \tag{34}$$

in terms of the sound speed $c_s(a)$, defined by

$$c_s(a) = \left[3\left(1 + \frac{3\Omega_{\text{b0}}}{4\Omega_{\gamma 0}}a\right)\right]^{-1/2}. \tag{35}$$

The seven-year WMAP observations gives $\Omega_{\gamma 0} = 2.469 \times 10^{-5} h^{-2}$ and $\Omega_{\text{b0}} = 0.02258^{+0.00057}_{-0.00056}$ [54].

The redshift of recombination z_* is obtained by using the fitting function proposed by Hu and Sugiyama [69]

$$z_* = 1048\left[1 + 0.00124(\Omega_{\text{b0}}h^2)^{-0.738}\right]\left[1 + g_1(\Omega_{\text{m0}}h^2)^{g_2}\right], \tag{36}$$

where

$$g_1 = \frac{0.0783(\Omega_{\text{b0}}h^2)^{-0.238}}{1 + 39.5(\Omega_{\text{b0}}h^2)^{0.763}}, \qquad g_2 = \frac{0.560}{1 + 21.1(\Omega_{\text{b0}}h^2)^{1.81}}. \tag{37}$$

Then one can define χ^2_{CMB} as $\chi^2_{\text{CMB}} = X^T C^{-1}_{\text{CMB}} X$, with [54]

$$X = \begin{pmatrix} l_A - 302.09 \\ R - 1.725 \\ z_* - 1091.3 \end{pmatrix}, \tag{38a}$$

$$C^{-1}_{\text{CMB}} = \begin{pmatrix} 2.305 & 29.698 & -1.333 \\ 293\,689 & 6825.270 & -113.180 \\ -1.333 & -113.180 & 3.414 \end{pmatrix}, \tag{38b}$$

where C^{-1}_{CMB} is the inverse covariant matrix.

To obtain χ^2_{SNIa}, the SNIa Union2 data [55] is used which includes 577 type Ia supernovae. The expansion history of the universe $H(z)$ can be given by a specific cosmological model. To test this model, we can use the observational data for some predictable cosmological parameter such as luminosity distance d_L. Assume that the Hubble parameter $H(z; \alpha_1, ..., \alpha_n)$ is used to describe the Universe, where parameters $(\alpha_1, ..., \alpha_n)$ are predicted by a theoretical cosmological model. For such a theoretical model we can predict the theoretical 'Hubble-constant free' luminosity distance as

$$D^{\text{th}}_L = H_0 \frac{d_L}{c} = (1+z) \int_0^z \frac{dz'}{E(z'; \alpha_z, ..., \alpha_n)}$$
$$= H_0 \frac{1+z}{\sqrt{|\Omega_k|}} \text{sinn} \left[\sqrt{|\Omega_k|} \int_0^z \frac{dz'}{H(z'; \alpha_z, ..., \alpha_n)} \right], \tag{39}$$

where $E \equiv H/H_0$, z is the redshift parameter, and

$$\text{sinn}(\sqrt{|\Omega_k|}x) = \begin{cases} \sin(\sqrt{|\Omega_k|}x) & \text{for } \Omega_k < 0 \\ \sqrt{|\Omega_k|}x & \text{for } \Omega_k = 0 \\ \sinh(\sqrt{|\Omega_k|}x) & \text{for } \Omega_k > 0. \end{cases}$$

Then one can write the theoretical modulus distance

$$\mu_{\text{th}}(z) = 5 \log_{10} \left[D^{\text{th}}_L(z) \right] + \mu_0, \tag{40}$$

where $\mu_0 = 5 \log_{10}(cH_0^{-1}/Mpc) + 25$. On the other hand, the observational modulus distance of SNIa, $\mu_{\text{obs}}(z_i)$, at redshift z_i is given by

$$\mu_{\text{obs}}(z_i) = m_{\text{obs}}(z_i) - M, \tag{41}$$

where m_{obs} and M are apparent and absolute magnitudes of SNIa respectively. Then the parameters of the theoretical model, α_is, can be determined by a likelihood analysis by defining $\bar{\chi}^2_{\text{SNIa}}(\alpha_i, M')$ in (30) as

$$\bar{\chi}^2_{\text{SNIa}}(\alpha_i, M') \equiv \sum_j \frac{(\mu_{\text{obs}}(z_j) - \mu_{\text{th}}(\alpha_i, z_j))^2}{\sigma_j^2}$$
$$= \sum_j \frac{(5 \log_{10}[D_L(\alpha_i, z_j)] - m_{\text{obs}}(z_j) + M')^2}{\sigma_j^2}, \tag{42}$$

where the nuisance parameter, $M' = \mu_0 + M$, can be marginalized over as

$$\chi^2_{\text{SNIa}}(\alpha_i) = -2 \ln \int_{-\infty}^{+\infty} dM' \exp \left[-\frac{1}{2} \chi^2_{\text{SNIa}}(\alpha_i, M') \right]. \tag{43}$$

Here we should mention an important point about using supernovae data to constrain the Brans–Dicke theories which have a varying gravitational coupling constant. Variations of gravitational coupling constant and apparent magnitude of supernovae are correlated as follows. The luminosity L of a supernova is powered by Nickel-35 mass which is proportional to the Chandrasekhar mass

$$L_{\text{SN}} \sim M_{\text{CH}} \sim G^{-3/2}. \tag{44}$$

Moreover, the luminosity distance d_L is the integral over the inverse Hubble parameter, which is proportional to $G^{-1/2}$. Therefore, the apparent magnitude m_{obs}

$$m_{\text{obs}} = -2.5 \log L + 5 \log d_L \tag{45}$$

varies with a change in the gravitational coupling constant ΔG as

$$\Delta m_{\text{obs}} \sim -\frac{1}{8} \frac{\Delta G}{G}. \tag{46}$$

On the other hand, in the Brans–Dicke theory we have

$$\frac{\dot{G}}{G} = -\frac{\dot{\phi}}{\phi} \tag{47}$$

where ϕ is the Brans–Dicke scalar field. In the slow roll approximation we can write

$$\dot{\phi} = H\epsilon(1 - q) \tag{48}$$

where q is the deceleration parameter. The average value of q between today and $z \sim 1.2$ (the redshift when the SN measurement are probing the dark energy) is of order unity, and by using $H = d \ln a / dt$, we can write

$$\frac{\Delta G}{G} \sim -\epsilon \Delta \ln a. \tag{49}$$

By using Eqs. (46) and (49) we obtain

$$\Delta m_{\text{obs}} \sim \frac{\epsilon}{8} \Delta \ln a. \tag{50}$$

In Union2 data set, the redshift interval is between 0.51 and 1.12, i.e. $\Delta \ln a \sim 1$, with the systematic error of order 0.03 in the measurement of apparent magnitude. Therefore, the systematic error can induce a bias roughly of order 0.3 on parameter ϵ, which is three order of magnitudes larger than the statistical errors, as we will discuss in the next section. Therefore, in order to constrain ϵ with a higher precision, we combine the supernovae data with other cosmological data sets as follows. For more detailed discussion on possible evolution of the gravitational constant from cosmological type Ia supernovae see [60].

The baryon acoustic oscillation data from the Sloan Digital Sky Survey (SDSS) Data Release 7 (DR7) [56] is used here for constraining model parameters. The data constrain parameter $d_z \equiv r_s(z_d)/D_V(z)$, where $r_s(z_d)$ is the comoving sound horizon distance (see (34)) at the drag epoch (where baryons were released from photons) and D_V is given by [70]

$$D_V(z) \equiv \left[c \left(\int_0^z \frac{dz'}{H(z')} \right)^2 \frac{z}{H(z)} \right]^{1/3}. \tag{51}$$

The drag redshift is given by the fitting formula [71]

$$z_d = \frac{1291(\Omega_{m0}h^2)^{0.251}}{1 + 0.659(\Omega_{m0}h^2)^{0.828}} \left[1 + b_1(\Omega_{b0}h^2)^{b_2} \right], \tag{52}$$

where

$$b_1 = 0.313(\Omega_{m0}h^2)^{-0.419} \left[1 + 0.607(\Omega_{m0}h^2)^{0.607} \right],$$
$$b_2 = 0.238(\Omega_{m0}h^2)^{0.223}. \tag{53}$$

Then we can obtain χ^2_{BAO} by $\chi^2_{\text{BAO}} = Y^T C^{-1}_{\text{BAO}} Y$, where

$$Y = \begin{pmatrix} d_{0.2} - 0.1905 \\ d_{0.35} - 0.1097 \end{pmatrix}, \tag{54}$$

Table 1
The best fit values of the cosmological and model parameters in the GDE model in the BD theory with 1σ and 2σ regions. Here CMB, SNIa and BAO and X-ray mass gas fraction data together with the BBN constraints have been used.

Parameter	Non-interacting	Interacting	Interacting non-flat
$\Omega_b h^2$	$0.0223^{+0.0016+0.0019}_{-0.0013-0.0018}$	$0.0224^{+0.0016+0.0018}_{-0.0016-0.0020}$	$0.0223^{+0.0018+0.0020}_{-0.0013-0.0017}$
$\Omega_c h^2$	$0.1149^{+0.0088+0.0104}_{-0.0104-0.0119}$	$0.1118^{+0.0117+0.0139}_{-0.0087-0.0101}$	$0.1151^{+0.0089+0.0098}_{-0.0132-0.0151}$
Ω_{DE}	$0.7148^{+0.0445+0.0535}_{-0.0356-0.0464}$	$0.7291^{+0.0360+0.0451}_{-0.0550-0.0700}$	$0.7133^{+0.0472+0.0552}_{-0.0386-0.0430}$
Ω_k	…	…	$0.0005^{+0.0025+0.0026}_{-0.0073-0.0073}$
ϵ	$0.0020^{+0.0004}_{-0.0006}$	$0.0017^{+0.0008}_{-0.0003}$	$0.0017^{+0.0007}_{-0.0003}$
ξ	…	$0.4895^{+0.3662+0.3769}_{-0.5951-0.5951}$	$0.6004^{+0.3638+0.3638}_{-0.6031-0.6065}$
H_0	$69.3902^{+4.3469+5.0061}_{-3.1604-3.6291}$	$70.4046^{+3.5815+4.1015}_{-4.2224-5.0097}$	$69.3060^{+4.2517+4.6106}_{-3.7536-4.5922}$
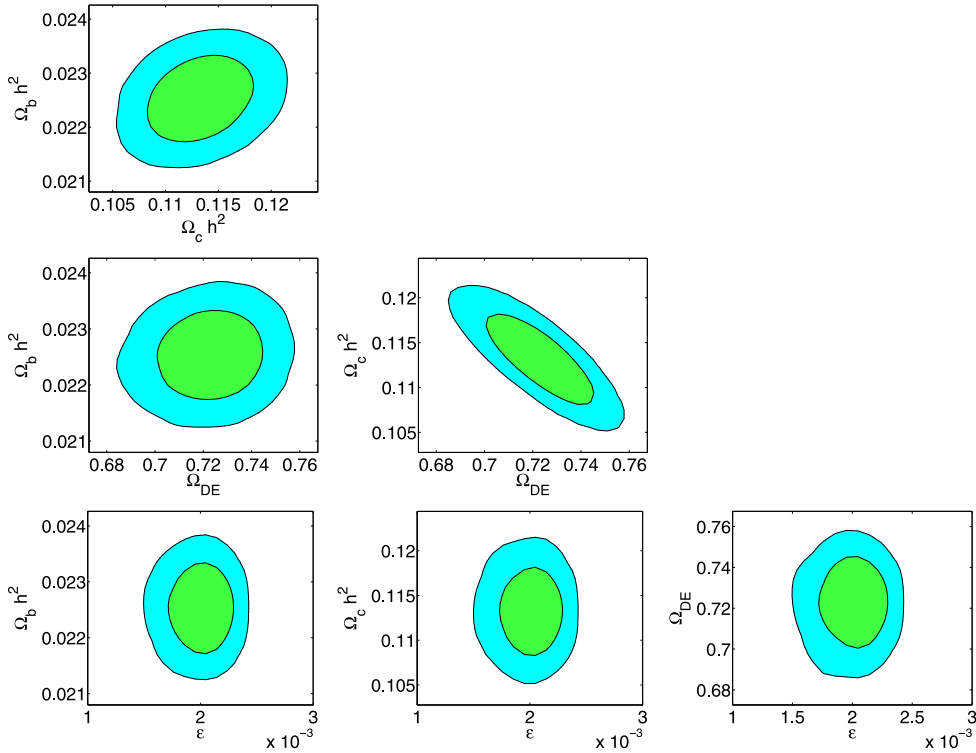
Fig. 1. 2-Dimensional constraint of the cosmological and model parameters contours in the flat non-interacting GDE model in the BD theory with 1σ and 2σ regions. To produce these plots, SNIa+CMB+BAO+X-ray gas mass fraction data together with the BBN constraints have been used.

and its covariance matrix is given by [56]

$$C_{BAO}^{-1} = \begin{pmatrix} 30\,124 & -17\,227 \\ -17\,227 & 86\,977 \end{pmatrix}. \tag{55}$$

The ratio of X-ray gas mass to the total mass of a cluster is defined as the X-ray gas mass fraction [57]. The model fitted to the ΛCDM model is [57]

$$f_{gas}^{\Lambda CDM}(z) = \frac{K A \gamma b(z)}{1 + s(z)} \left(\frac{\Omega_b}{\Omega_{m0}} \right) \left(\frac{D_A^{\Lambda CDM}(z)}{D_A(z)} \right)^{1.5}. \tag{56}$$

The elements in Eq. (60) are defined as follows: $D_A^{\Lambda CDM}(z)$ and $D_A(z)$ are the proper angular diameter distance in ΛCDM and the alternative theoretical model respectively, where

$$D_A(z) = \frac{c}{(1+z)\sqrt{|\Omega_k|}} sinn \left[\sqrt{|\Omega_k|} \int_0^z \frac{dz'}{H(z')} \right]. \tag{57}$$

The angular correction factor A

$$A = \left(\frac{\theta_{2500}^{\Lambda CDM}}{\theta_{2500}} \right)^{\eta} \approx \left(\frac{H(z) D_A(z)}{[H(z) D_A(z)]^{\Lambda CDM}} \right)^{\eta}, \tag{58}$$

is caused by changes in angle for the alternative theoretical model θ_{2500} compared to $\theta_{2500}^{\Lambda CDM}$, where $\eta = 0.214 \pm 0.022$ [57] is the slope of the $f_{gas}(r/r_{2500})$ data within the radius r_{2500} (r_{2500} is the radius of the gas core in Mpc/h units).

The bias factor $b(z)$ in Eq. (60) contains information about the uncertainties in the cluster depletion factor $b(z) = b_0(1 + \alpha_b z)$ and the parameter γ accounts for departures from the hydrostatic equilibrium. The function $s(z) = s_0(1 + \alpha_s z)$ denotes the uncertainties of the baryonic mass fraction in stars with a Gaussian prior for s_0, with $s_0 = (0.16 \pm 0.05)h_{70}^{0.5}$ [57]. The factor K describes the combined effects of the residual uncertainties, such as the instrumental calibration. A Gaussian prior for the 'calibration' factor is considered as $K = 1.0 \pm 0.1$ [57].

Then χ_{gas}^2 is defined as [57]

$$\chi_{gas}^2 = \sum_i^N \frac{[f_{gas}^{\Lambda CDM}(z_i) - f_{gas}(z_i)]^2}{\sigma_{f_{gas}}^2(z_i)} + \frac{(s_0 - 0.16)^2}{0.0016^2}$$
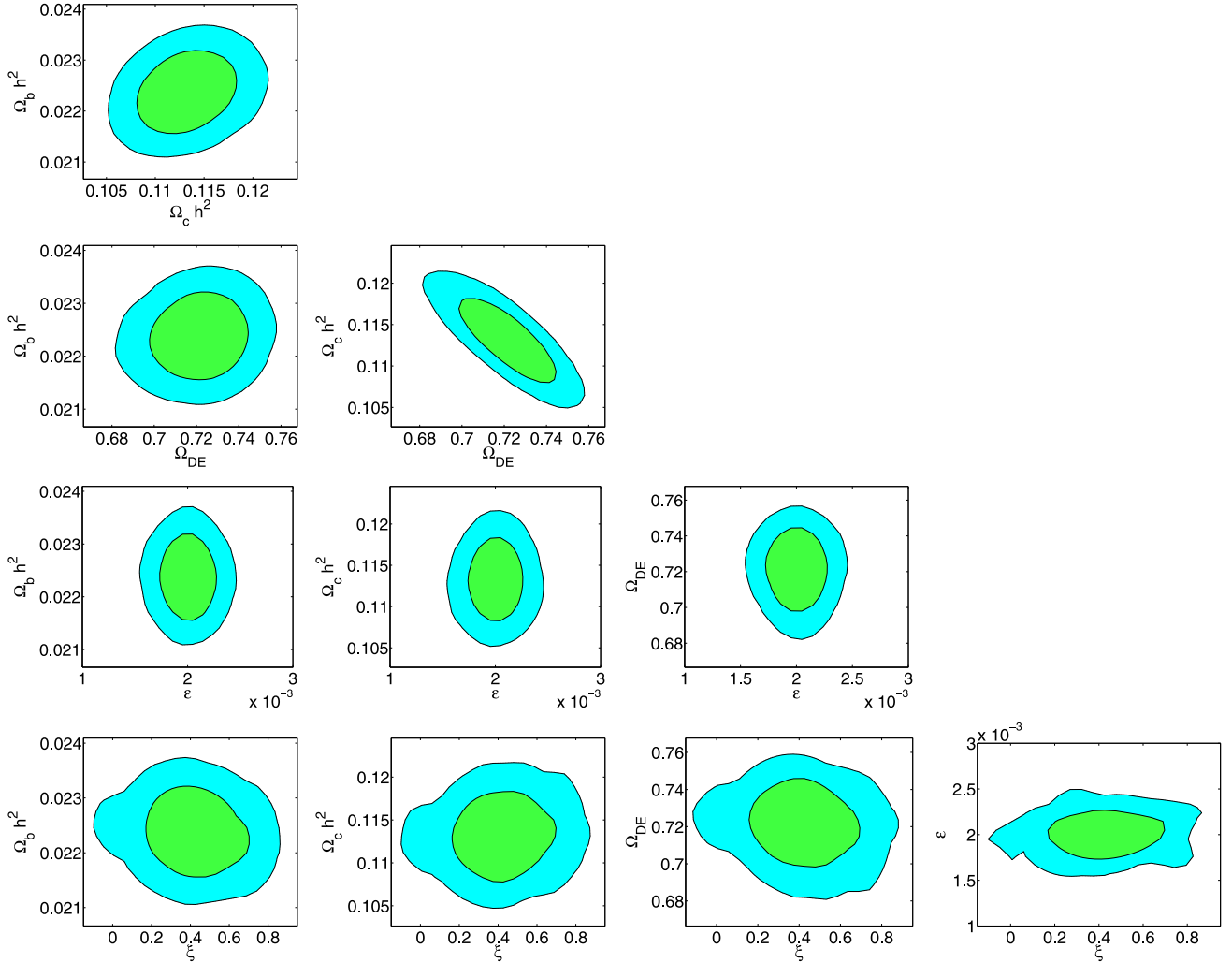
Fig. 2. 2-Dimensional constraint of the cosmological and model parameters contours in the flat interacting GDE model in the BD theory with 1σ and 2σ regions. To produce these plots, SNIa+CMB+BAO+X-ray gas mass fraction data together with the BBN constraints have been used.

$$+ \frac{(K - 1.0)^2}{0.01^2} + \frac{(\eta - 0.214)^2}{0.022^2}, \tag{59}$$

with the statistical uncertainties $\sigma_{f_{gas}}(z_i)$ and

$$f_{gas}(z) = \frac{K A \gamma b(z)}{1 + s(z)} \left(\frac{\Omega_b}{\Omega_{m0}} \right) \left(\frac{D_A^{\Lambda CDM}(z)}{D_A(z)} \right)^{1.5}. \tag{60}$$

At the end of this section we should assert that the data points parameters of the CMB and BAO data sets which we use in this paper are the best fit values for ΛCDM and the error estimates are also based on the ΛCDM model. Therefore they are not completely accurate in this application. However they are the only parameters which we have to constrain our model.

4. Results

Finally we apply a Markov chain Monte Carlo simulation on the parameters of the GDEBD model by using the publicly available CosmoMC code [72]. The parameter vectors are $P_s^{I} = \{\Omega_b h^2, \Omega_c h^2, \epsilon\}$, $P_s^{II} = \{\Omega_b h^2, \Omega_c h^2, \epsilon, \xi\}$, $P_s^{III} = \{\Omega_b h^2, \Omega_c h^2, \epsilon, \xi, \Omega_k\}$ for the flat non-interacting (model I), flat interacting (model II) and non-flat interacting (model III) models respectively. The basic cosmological parameters are taken in the following priors: $\Omega_b h^2 = [0.005 \, 0.9]$, $\Omega_c h^2 = [0.01, 0.99]$ and $\Omega_k = [-0.05, 0.05]$. In addition, as we mentioned in Section 2, for the

model fitting, we consider $\omega\varepsilon = 1$ condition. The results are presented in Table 1 and Figs. 1–3.

From Table 1 one can see that the main cosmological parameters $\Omega_b h^2$, $\Omega_c h^2$, Ω_{DE} and Ω_k in all three models are compatible with the results of the ΛCDM model [61]. In addition, in the presence of interaction between DM and DE, the parameter ϵ decreases and so the Brans–Dicke parameter ω increases. The best fit value of the parameter $\epsilon = 1/\omega$ in all three models is compatible with the results of other cosmological constraining works (however see the discussion following Eq. (43)). For example in [47] the authors by using the CMB temperature and polarization anisotropy data, found $1/\omega \simeq 0.001$. Wu and Chen in [50,51] by using the five-year WMAP and SDSS data obtained $\omega > 97.8$. For other cosmological constraints on the BD theory see [48,49,73–76]. This estimated value is also compatible with the results of the solar system tests of the scalar-tensor theories such as the Cassini experiment where it has been obtained $\omega > 10^4$ [46,48]. The positive best fit value of parameter ξ describe a conversion of dark matter to dark energy although both in flat and non-flat universes, in 1-σ CL, an inverse conversion is possible as well. The interacting DE and DM models have been constrained by observational data by many authors with different parametrization of the interacting parameter Q [77–83]. He et al. in [82] have parametrized the interaction parameter as in the present paper although they have chosen the prior on parame-
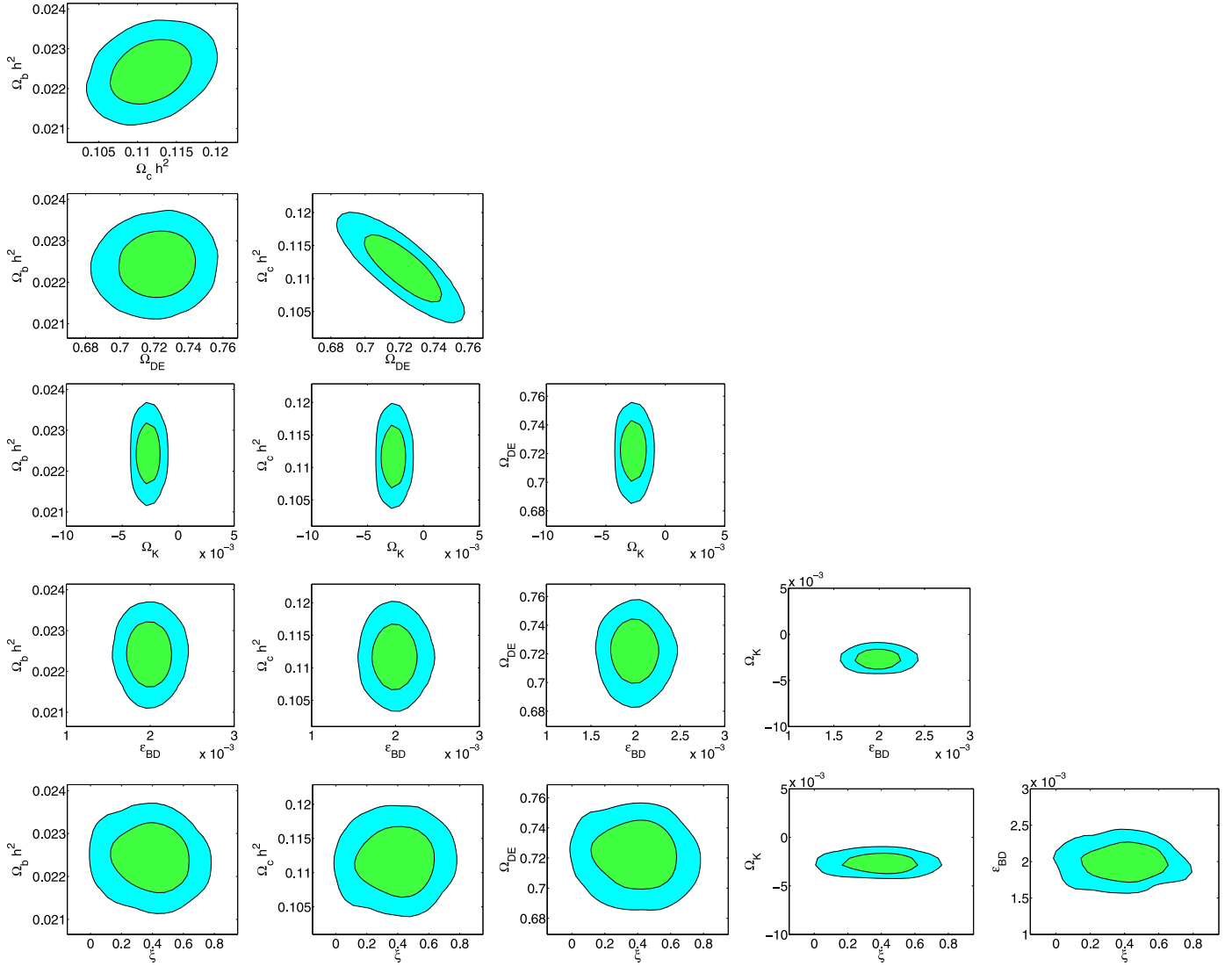
Fig. 3. 2-Dimensional constraint of the cosmological and model parameters contours in the non-flat interacting GDE model in the BD theory with 1σ and 2σ regions. To produce these plots, SNIa+CMB+BAO+X-ray gas mass fraction data together with the BBN constraints have been used.

ter ξ as $\xi = [0, 0.02]$. They obtained the best fit value of parameter ξ as $\xi = 0.0006 \pm 0.0006$.

5. Conclusion

In this paper we considered the cosmological constraints on the parameters of the GDE in the framework of BD theory by using a Markov Chain Monte Carlo simulation. We used the SNIa+CMB+BAO+X-ray gas mass fraction data for the model fitting. The best fit values of the cosmological parameters in this model are compatible with the results of the ΛCDM model. In addition, we obtained the best fit values of parameters $\epsilon = 1/\omega$ and ξ where ω is the BD parameter and ξ is the interacting parameter. The best fit values of these parameters are also compatible with the results of previous constraining works. However as we mentioned in Section 3, due to large systematic error in ϵ by using the supernovae data only, to constrain this parameter with a higher precision, we should combine the supernovae data with other cosmological data sets as the CMB and BAO data sets. In addition we should assert one more time that the data points parameters of the CMB and BAO data which we have used in this paper are the best fit values for ΛCDM and the error estimates are also based

on the ΛCDM model. Therefore they are not completely accurate in this application. The numerical results can be improved in the future works by using more recent data such as nine-year WMAP [61] or the Planck [84] projects.

References

[1] A.G. Riess, et al., Observational evidence from supernovae for an accelerating universe and a cosmological constant, Astron. J. 116 (1998) 1009–1038.
[2] S. Perlmutter, et al., Measurements of ω and λ from 42 high redshift supernovae, Astrophys. J. 517 (1999) 565–586.
[3] C. Wetterich, Cosmology and the fate of dilatation symmetry, Nucl. Phys. B 302 (1988) 668.
[4] B. Ratra, P. Peebles, Cosmological consequences of a rolling homogeneous scalar field, Phys. Rev. D 37 (1988) 3406.

[5] C. Armendariz-Picon, V.F. Mukhanov, P.J. Steinhardt, A dynamical solution to the problem of a small cosmological constant and late time cosmic acceleration, Phys. Rev. Lett. 85 (2000) 4438–4441.

[6] C. Armendariz-Picon, V.F. Mukhanov, P.J. Steinhardt, Essentials of k essence, Phys. Rev. D 63 (2001) 103510.

[7] T. Padmanabhan, Accelerated expansion of the universe driven by tachyonic matter, Phys. Rev. D 66 (2002) 021301.

[8] A. Sen, Tachyon matter, J. High Energy Phys. 0207 (2002) 065.

[9] R. Caldwell, A Phantom menace?, Phys. Lett. B 545 (2002) 23–29.

[10] S. Nojiri, S.D. Odintsov, Quantum de Sitter cosmology and phantom matter, Phys. Lett. B 562 (2003) 147–152.

[11] S. Nojiri, S.D. Odintsov, De Sitter brane universe induced by phantom and quantum effects, Phys. Lett. B 565 (2003) 1–9.

[12] N. Arkani-Hamed, H.-C. Cheng, M.A. Luty, S. Mukohyama, Ghost condensation and a consistent infrared modification of gravity, J. High Energy Phys. 0405 (2004) 074.

[13] F. Piazza, S. Tsujikawa, Dilatonic ghost condensate as dark energy, J. Cosmol. Astropart. Phys. 0407 (2004) 004.

[14] E. Elizalde, S. Nojiri, S.D. Odintsov, Late-time cosmology in (phantom) scalar-tensor theory: dark energy and the cosmic speed-up, Phys. Rev. D 70 (2004) 043539.

[15] S. Nojiri, S.D. Odintsov, S. Tsujikawa, Properties of singularities in (phantom) dark energy universe, Phys. Rev. D 71 (2005) 063004.

[16] A. Anisimov, E. Babichev, A. Vikman, B-inflation, J. Cosmol. Astropart. Phys. 0506 (2005) 006.

[17] E. Witten, The Cosmological Constant from the Viewpoint of String Theory, 2000, pp. 27–36.

[18] R.-G. Cai, A dark energy model characterized by the age of the universe, Phys. Lett. B 657 (2007) 228–231.

[19] H. Wei, R.-G. Cai, A new model of agegraphic dark energy, Phys. Lett. B 660 (2008) 113–117.

[20] E.J. Copeland, M. Sami, S. Tsujikawa, Dynamics of dark energy, Int. J. Mod. Phys. D 15 (2006) 1753–1936.

[21] M. Li, X.-D. Li, S. Wang, Y. Wang, Dark energy, Commun. Theor. Phys. 56 (2011) 525–604.

[22] A. De Felice, S. Tsujikawa, $f(R)$ theories, Living Rev. Relativ. 13 (2010) 3.

[23] G. Dvali, G. Gabadadze, M. Porrati, 4-D gravity on a brane in 5-D Minkowski space, Phys. Lett. B 485 (2000) 208–214.

[24] M.S. Carena, J. Lykken, M. Park, J. Santiago, Self-accelerating warped braneworlds, Phys. Rev. D 75 (2007) 026009.

[25] M. Minamitsuji, Self-accelerating solutions in cascading DGP braneworld, Phys. Lett. B 684 (2010) 92–95.

[26] A. Sheykhi, B. Wang, N. Riazi, String inspired explanation for the super-acceleration of our universe, Phys. Rev. D 75 (2007) 123513.

[27] K. Kawarabayashi, N. Ohta, The problem of η in the large N limit: effective Lagrangian approach, Nucl. Phys. B 175 (1980) 477.

[28] E. Witten, Current algebra theorems for the $U(1)$ Goldstone boson, Nucl. Phys. B 156 (1979) 269.

[29] G. Veneziano, $U(1)$ without instantons, Nucl. Phys. B 159 (1979) 213–224.

[30] C. Rosenzweig, J. Schechter, C. Trahern, Is the effective Lagrangian for QCD a sigma model?, Phys. Rev. D 21 (1980) 3388.

[31] N. Ohta, Dark energy and QCD ghost, Phys. Lett. B 695 (2011) 41–44.

[32] F.R. Urban, A.R. Zhitnitsky, The cosmological constant from the QCD Veneziano ghost, Phys. Lett. B 688 (2010) 9–12.

[33] R.-G. Cai, Z.-L. Tuo, H.-B. Zhang, Q. Su, Notes on ghost dark energy, Phys. Rev. D 84 (2011) 123501.

[34] A. Sheykhi, M. Sadegh Movahed, Interacting ghost dark energy in non-flat universe, Gen. Relativ. Gravit. 44 (2012) 449–465.

[35] E. Ebrahimi, A. Sheykhi, Instability of QCD ghost dark energy model, Int. J. Mod. Phys. D 20 (2011) 2369–2381.

[36] A. Sheykhi, M. Sadegh Movahed, E. Ebrahimi, Tachyon reconstruction of ghost dark energy, Astrophys. Space Sci. 339 (2012) 93–99.

[37] A. Sheykhi, A. Bagheri, Quintessence ghost dark energy model, Europhys. Lett. 95 (2011) 39001.

[38] A. Sheykhi, Viscous ghost dark energy with a varying gravitational constant, Phys. Scr. 85 (2012) 045901.

[39] A. Rozas-Fernandez, Kinetic k-essence ghost dark energy model, Phys. Lett. B 709 (2012) 313–321.

[40] K. Karami, M. Mousivand, S. Asadzadeh, Z. Safari, QCD modified ghost scalar field dark energy models, Int. J. Mod. Phys. D 22 (2013) 1350018.

[41] A. Khodam-Mohammadi, M. Malekjani, Reconstruction of modified gravity with ghost dark energy models, Mod. Phys. Lett. A 27 (2012) 1250100.

[42] M. Malekjani, A. Khodam-Mohammadi, Statefinder diagnosis and the interacting ghost model of dark energy, Astrophys. Space Sci. 343 (2013) 451–461.

[43] C.-J. Feng, X.-Z. Li, X.-Y. Shen, Latest observational constraints to the ghost dark energy model by using Markov chain Monte Carlo approach, Phys. Rev. D 87 (2013) 023006.

[44] R.-G. Cai, Z.-L. Tuo, Y.-B. Wu, Y.-Y. Zhao, More on QCD ghost dark energy, Phys. Rev. D 86 (2012) 023511.

[45] C. Brans, R. Dicke, Mach's principle and a relativistic theory of gravitation, Phys. Rev. 124 (1961) 925–935.

[46] B. Bertotti, L. Iess, P. Tortora, A test of general relativity using radio links with the Cassini spacecraft, Nature 425 (2003) 374.

[47] X.-l. Chen, M. Kamionkowski, Cosmic microwave background temperature and polarization anisotropy in Brans–Dicke cosmology, Phys. Rev. D 60 (1999) 104036.

[48] V. Acquaviva, L. Verde, Observational signatures of Jordan–Brans–Dicke theories of gravity, J. Cosmol. Astropart. Phys. 0712 (2007) 001.

[49] S. Tsujikawa, K. Uddin, S. Mizuno, R. Tavakol, J. Yokoyama, Constraints on scalar-tensor models of dark energy from observational and local gravity tests, Phys. Rev. D 77 (2008) 103009.

[50] F. Wu, X. Chen, Cosmic microwave background with Brans–Dicke gravity II: constraints with the WMAP and SDSS data, Phys. Rev. D 82 (2010) 083003.

[51] F. Wu, X. Chen, Constraints on the Brans–Dicke gravity theory with the Planck data, Phys. Rev. D 88 (2013) 084053.

[52] E. Ebrahimi, A. Sheykhi, Interacting ghost dark energy in Brans–Dicke theory, Phys. Lett. B 706 (2011) 19–25.

[53] K. Saaidi, Stability of Ghost Dark Energy in CBD Model of Gravity, 2012.

[54] E. Komatsu, et al., Seven-year Wilkinson Microwave Anisotropy Probe (WMAP) observations: cosmological interpretation, Astrophys. J. Suppl. Ser. 192 (2011) 18.

[55] R. Amanullah, C. Lidman, D. Rubin, G. Aldering, P. Astier, et al., Spectra and light curves of six type Ia supernovae at $0.511 < z < 1.12$ and the Union2 compilation, Astrophys. J. 716 (2010) 712–738.

[56] W.J. Percival, et al., Baryon acoustic oscillations in the Sloan digital sky survey data release 7 galaxy sample, Mon. Not. R. Astron. Soc. 401 (2010) 2148–2168.

[57] S. Allen, D. Rapetti, R. Schmidt, H. Ebeling, G. Morris, et al., Improved constraints on dark energy from Chandra X-ray observations of the largest relaxed galaxy clusters, Mon. Not. R. Astron. Soc. 383 (2008) 879–896.

[58] A. Lewis, S. Bridle, Cosmological parameters from CMB and other data: a Monte Carlo approach, Phys. Rev. D 66 (Nov 2002) 103511.

[59] M. Arik, M. Calik, Can Brans–Dicke scalar field account for dark energy and dark matter?, Mod. Phys. Lett. A 21 (2006) 1241–1248.

[60] E. Gaztanaga, E. Garcia-Berro, J. Isern, E. Bravo, I. Dominguez, Phys. Rev. D 65 (2002) 023506.

[61] C. Bennett, et al., Nine-Year Wilkinson Microwave Anisotropy Probe (WMAP) Observations: Final Maps and Results, 2012.

[62] O. Bertolami, F. Gil Pedro, M. Le Delliou, Dark energy-dark matter interaction and the violation of the equivalence principle from the abell cluster A586, Phys. Lett. B 654 (2007) 165–169.

[63] S. Tsujikawa, M. Sami, A unified approach to scaling solutions in a general cosmological background, Phys. Lett. B 603 (2004) 113–123.

[64] N. Banerjee, D. Pavon, Holographic dark energy in Brans–Dicke theory, Phys. Lett. B 647 (2007) 477–481.

[65] A. Sheykhi, Interacting holographic dark energy in Brans–Dicke theory, Phys. Lett. B 681 (2009) 205–209.

[66] C.M. Will, Theory and Experiment in Gravitational Physics, 2nd ed., Basic Books/Perseus Group, New York, 1993.

[67] R.A. Daly, S. Djorgovski, K.A. Freeman, M.P. Mory, C. O'Dea, et al., Improved constraints on the acceleration history of the universe and the properties of the dark energy, Astrophys. J. 677 (2008) 1–11.

[68] J. Bond, G. Efstathiou, M. Tegmark, Forecasting cosmic parameter errors from microwave background anisotropy experiments, Mon. Not. R. Astron. Soc. 291 (1997) L33–L41.

[69] W. Hu, N. Sugiyama, Small scale cosmological perturbations: an analytic approach, Astrophys. J. 471 (1996) 542–570.

[70] D.J. Eisenstein, et al., Detection of the baryon acoustic peak in the large-scale correlation function of SDSS luminous red galaxies, Astrophys. J. 633 (2005) 560–574.

[71] D.J. Eisenstein, W. Hu, Baryonic features in the matter transfer function, Astrophys. J. 496 (1998) 605.

[72] A. Lewis, S. Bridle, Cosmological parameters from CMB and other data: a Monte Carlo approach, Phys. Rev. D 66 (2002) 103511.

[73] R. Nagata, T. Chiba, N. Sugiyama, Observational consequences of evolution of primordial fluctuations in scalar-tensor cosmology, Phys. Rev. D 66 (2002) 103510.

[74] R. Nagata, T. Chiba, N. Sugiyama, WMAP constraints on scalar-tensor cosmology and the variation of the gravitational constant, Phys. Rev. D 69 (2004) 083512.

[75] V. Acquaviva, C. Baccigalupi, S.M. Leach, A.R. Liddle, F. Perrotta, Structure formation constraints on the Jordan–Brans–Dicke theory, Phys. Rev. D 71 (2005) 104025.

[76] C. Schimd, J.-P. Uzan, A. Riazuelo, Weak lensing in scalar-tensor theories of gravity, Phys. Rev. D 71 (2005) 083512.

[77] L.P. Chimento, A.S. Jakubi, D. Pavon, W. Zimdahl, Interacting quintessence solution to the coincidence problem, Phys. Rev. D 67 (2003) 083513.

[78] W. Zimdahl, D. Pavon, Scaling cosmology, Gen. Relativ. Gravit. 35 (2003) 413–422.

[79] J. Valiviita, R. Maartens, E. Majerotto, Observational constraints on an interacting dark energy model, Mon. Not. R. Astron. Soc. 402 (2010) 2355–2368.

[80] V. Pettorino, L. Amendola, C. Baccigalupi, C. Quercellini, Constraints on coupled dark energy using CMB data from WMAP and SPT, Phys. Rev. D 86 (2012) 103507.

[81] V. Salvatelli, A. Marchini, L. Lopez-Honorez, O. Mena, New constraints on coupled dark energy from the Planck satellite experiment, Phys. Rev. D 88 (2013) 023531.

[82] J.-H. He, B. Wang, E. Abdalla, Testing the interaction between dark energy and dark matter via latest observations, Phys. Rev. D 83 (2011) 063515.

[83] T. Clemson, K. Koyama, G.-B. Zhao, R. Maartens, J. Valiviita, Interacting dark energy – constraints and degeneracies, Phys. Rev. D 85 (2012) 043007.

[84] P. Ade, et al., Planck 2013 results. XVI. Cosmological parameters, arXiv:1303.5076 [astro-ph.CO], 2013.